BBA - Molecular Basis of Disease 1865 (2019) 445–453

Contents lists available at ScienceDirect

BBA - Molecular Basis of Disease

journal homepage: www.elsevier.com/locate/bbadis

Troglitazone activates TRPV1 and causes deacetylation of PPARγ in 3T3-L1 cells

Vivek Krishnan[1], Padmamalini Baskaran[1], Baskaran Thyagarajan[*]

Molecular Signaling Laboratory, School of Pharmacy, University of Wyoming, Laramie, WY 82071, United States of America

ARTICLE INFO

Keywords:
TRPV1
3T3-L1 cells
Troglitazone
PPARs
Sirtuin 1
Epididymal fat

ABSTRACT

Published research suggests that activation of transient receptor potential vanilloid subfamily 1 (TRPV1) enhances the expression and deacetylation of peroxisome proliferator-activated receptor gamma (PPARγ) to cause browning of white adipose tissue. Here, we show that TRPV1 activation by capsaicin significantly prevents high fat diet-induced obesity in mice. This is associated with an increase in the expression and deacetylation of PPARγ in the epididymal fat of these mice. Consistent with the TRPV1 activation in vivo, overexpression of TRPV1 enhanced the PPARγ and other thermogenic genes in cultured 3T3-L1 preadipocytes. To determine the interaction between TRPV1 and PPARγ signaling, we analyzed the effect of Troglitazone (Trog; a thiazolidinedione derivative and an agonist of PAARγ) treatment on cultured 3T3-L1 cells. Trog enhanced the expression of TRPV1, PPARγ and thermogenic proteins in undifferentiated 3T3-L1 cells but not in differentiated cells. Acute application of Trog stimulated a robust Ca^{2+} influx into 3T3-L1 cells and TRPV1 inhibition by capsazepine prevented this. More interestingly, Trog or capsaicin treatment caused the deacetylation of PPARγ in 3T3-L1 cells and inhibition of TRPV1 or Sirtuin 1 - prevented this. Our data suggest a novel effect of Trog to induce PPARγ deacetylation by activating TRPV1. This research has a significant implication on the role of TRPV1 and PPARγ signaling in the browning of white adipose tissue.

1. Introduction

The interaction between transient receptor potential vanilloid subfamily 1 (TRPV1) and peroxisome proliferator-activated receptors alpha and gamma (PPARα and PPARγ) signaling has received significant attention in human diseases. Specifically, the activation of TRPV1 enhances the expression of PPARγ in white and brown adipose tissue (WAT and BAT) and stimulates post-translational deacetylation of PPARγ to induce the browning of WAT and BAT thermogenesis.

Peroxisome proliferator-activated receptors (PPARs) are ligand-dependent transcription factors that regulate lipid homeostasis [1] and PPAR isoforms regulate lipolysis, adipogenesis, and metabolism [2]. Interestingly, posttranslational modifications of PPARγ, especially its deacetylation, have been recognized as a marker for browning of white adipose tissue (WAT). Direct acetylation of PPARγ by histone acetyltransferases is involved in its adipocyte differentiation function [3]. PPARγ acetylation enhances lipid synthesis, and the deacetylation of PPARγ is tightly regulated by NAD-dependent deacetylase sirtuin 1 [SiRT1; [4,5]].

It is well known that WAT functions as the main depot for fuel storage whereas brown fat dissipates this energy as heat [6] and increases energy expenditure, thus preventing from obesity. The third kind of fat shown recently is inducible brown fat in white fat also called as beige/brite (brown in white) cells [7]. Previous research also shows that brown remodeling of white adipose tissue occurs by SiRT1-dependent deacetylation of PPARγ and inhibits lipid accumulation [5]. Recent research has intensified the identification of various mechanisms that trigger the browning of WAT as a countermeasure for obesity.

Transient receptor potential vanilloid subfamily 1 (TRPV1) is a nonselective cation channel [8], which takes part in nociception, thermosensation, and release of vasodilator neuropeptides such as calcitonin gene-related peptide [9]. It was recently shown that TRPV1

Abbreviations: Trog, Troglitazone; CLO, Clofibrate; TRPV1, transient receptor potential vanilloid subfamily 1; PPARs, peroxisome proliferator-activated receptors; PGC-1α, PPARγ coactivator 1α; SiRT-1, Sirtuin 1; BMP8b, bone morphogenetic protein 8b; UCP-1, uncoupling protein 1; CAP, capsaicin; CPZ, capsazepine; EF, epididymal fat; HFD, high fat diet; WAT, white adipose tissue; BAT, brown adipose tissue

* Corresponding author at: University of Wyoming, College of Health Sciences, Dept. 3375, 1000 East University Avenue, Laramie, WY 82071, United States of America.

E-mail address: bthyagar@uwyo.edu (B. Thyagarajan).

[1] Equal contribution.

https://doi.org/10.1016/j.bbadis.2018.11.004
Received 29 July 2018; Received in revised form 18 October 2018; Accepted 5 November 2018
Available online 26 November 2018

channel activation prevents adipogenesis [10]. More significantly, the activation of TRPV1 by feeding capsaicin prevented high-fat diet-induced obesity [11], promoted weight loss and induced the conversion of white to brown fat in mice. Also, capsaicin enhanced the expression and thermogenic program in the brown fat of wild-type but not in TRPV1$^{-/-}$ mice. TRPV1 activation caused the deacetylation of PPARγ via SiRT-1 in white and brown adipose tissues [11,12]. In this study, we evaluated the crosstalk between TRPV1 and PPARγ by evaluating the effect of Troglitazone (Trog), a PPARγ activator. Our data suggest a novel TRPV1-dependent effect of Trog on the deacetylation of PPARγ in 3T3-L1 cells.

2. Materials and methods

2.1. Mouse model of HFD-induced obesity

Adult male TRPV1$^{-/-}$ mice (stock number 003770) and their genetically unaltered wild-type control mice were purchased from Jackson Laboratory, Maine, USA, and housed in the research animal facility. Mice were maintained at 23 °C with 12:12 hour dark and light cycle, at the School of Pharmacy, University of Wyoming and used for experiments as per approved IACUC protocols. Mice were allowed access to the high-fat diet (HFD; 60% calories from fat; 5.24 kCal/g) or HFD + CAP (0.01% in HFD) and water ad libitum.

2.1.1. Group size and randomization

Six-week -old male mice (n = 8 to 12 per group) were randomly assigned to feeding groups and housed in groups of four in separate cages. The study design and animal ethics conform to the recent guidance on experimental design and analysis [13]. Mice received NCD or HFD (± 0.01% CAP in total diet) from week 6 through 38. At the end of 32 weeks of feeding the diets, epididymal fat (EF) was isolated and used for quantitative RT PCR and western blotting as per previously described procedures [11,12].

2.1.2. Blinding

The average weight gain was determined on a weekly basis. The weighing personnel was blinded on the groups of mice that were fed NCD, HFD or HFD + CAP.

2.2. Cell culture

Murine 3T3-L1 cells were grown in Dulbecco's modified essential medium (DMEM) containing 10% fetal calf serum and 1% penicillin and streptomycin. Control and TRPV1 overexpressing HEK 293 ells were cultured in MEM containing 10% fetal bovine serum and 1% penicillin and streptomycin.

2.3. Differentiation of 3T3-L1 cells

For differentiation, confluent 3T3-L1 cells were treated with 0.5 mM isobutyl methylxanthine, 1 μM dexamethasone and 20 μg/mL insulin (differentiation medium). After 48 h, the medium was aspirated and insulin and FBS containing DMEM complete medium was added. This procedure continued every day till 8-days after inducing differentiation.

2.4. Oil red O staining protocol

3T3-L1 cells were washed three times with phosphate buffered saline (PBS) and then fixed with 10% formaldehyde for 10 min. The cells were treated with 100% polyethylene glycol for 2 min followed by oil red O in polyethylene glycol for 15 min. The oil red O was removed and 60% polyethylene glycol was added for 1 min. The cells were then rinsed with water and the nucleus was stained with hematoxylin for 10 min. The nuclear staining was intensified with sodium phosphate solution for 5 min. The coverslips were washed with water several times and mounted using aqueous mounting medium. The cells were visualized using a Zeiss 710 confocal microscope.

2.5. Quantification of lipid content in 3T3L1 cells

For quantification of content, cells were fixed for at least 1 h with 10% formalin in isotonic phosphate buffer, then washed with water, stained for 2 h by complete immersion in a working solution of oil red O and exhaustively rinsed with water. Excess water was removed by placing the stained cultures at 32 °C. Then 1 mL of isopropyl alcohol was added to the stained culture dish, the extracted dye was immediately removed by gentle pipetting and its absorbance monitored spectrophotometrically at 510 nm. The working solution of oil red O was prepared as described previously [14]. The cells were then scraped and lysed and protein concentration was determined by Bradford method and absorbance was calculated for the protein concentration/dish.

2.6. Transfection of TRPV1

3T3-L1 cells were grown to confluence and transfected with rat transient receptor potential vanilloid subfamily 1 (TRPV1) cDNA or pcDNA3.1 vector using Effectene transfection reagent (Qiagen, Valencia, CA) following the manufacturer's instructions. We also used TRPV1 stably expressing HEK293 cells [12,15] as controls for mRNA and protein expression analyses of TRPV1 in 3T3-L1 cells.

2.7. Isolation and culture of EF adipocytes

The EF pads were isolated from 8 to 10 weeks old NCD-fed WT and TRPV1$^{-/-}$ mice and minced in 500 μL ice-cold sterile PBS. Collagenase (0.5 mL of 1.5 mg·mL^{-1}) in isolation buffer (123 mM NaCl, 5 mM KCl, 1.3 mM $CaCl_2$, 5 mM glucose, HEPES 100 mM, 1% penicillin and streptomycin), and 4% BSA (fraction V) were added and incubated in shaking water bath at 37 °C for 45 min, with 10 s vortexing for every 5 min. The digested tissues were filtered (100 μm filter) and centrifuged at 370 × g for 5 min. The pellet was suspended in 1 mL of red blood cell lysis buffer for 1 min. Sterile PBS (9 mL) was added and filtered (70 μm filter). The pellet was resuspended in DMEM (high glucose) containing 20% FBS, 20 mM HEPES and 1% penicillin and streptomycin and added to 1% gelatin-coated plates for 45 min to remove the fibroblasts. The supernatant was then seeded in treated cell culture plates and used for intracellular Ca^{2+} imaging experiments 24 h after plating.

2.8. Intracellular Ca^{2+} measurement

For intracellular Ca^{2+} imaging, undifferentiated or differentiated 3T3-L1 cells or epididymal adipocytes isolated from NCD-fed WT and TRPV1$^{-/-}$ mice grown on 25 mm circular coverslips were incubated with Fura-2AM (2 μM; for 60 min) at room temperature in an extracellular buffer containing in mM, NaCl 137, KCl 5, $CaCl_2$ 1.8, $MgCl_2$ 1, HEPES 10, glucose 10, pH 7.38. The coverslips were then washed with buffer, placed in a stainless-steel holder (0.8 mL residual volume), and viewed with a Leica DMI3000 B inverted microscope coupled to a Polychrome V digital imaging system equipped with Imago CCD camera. Cells were continuously superfused (22 °C) with buffer, and Ca^{2+} entry due to the addition of CAP (1 μM), Trog (10 μM), Rosi (10 μM) or CLO (10 μM) in the presence of 2 mM extracellular Ca^{2+} containing buffer was measured. Results were analyzed using TillVision 5 software and presented as the ratio (R) of fluorescence intensities at excitation wavelengths of 340 nm and 380 nm collected at 510 nm. For the inhibition of TRPV1, CPZ (10 μM) was added to cells prior to adding Trog (10 μM).

2.9. Western blotting

Cultured 3T3-L1^{TRPV1} cells or EF tissues were washed with chilled PBS, lysed in lysis buffer (50 mM Tris pH 7.5, 250 mM sodium chloride, 0.5% NP40, 0.5% sodium deoxycholate, 2 mM EDTA, 0.5 mM DTT, 1 mM sodium orthovanadate, Protease inhibitor cocktail) and centrifuged at 14,000 rpm for 20 min to remove the cell debris. The supernatants were aliquoted and snap-frozen in liquid nitrogen. The protein concentration was determined using the Bradford method and equal amounts of protein were separated by SDS-PAGE and transferred to nitrocellulose membrane, and immunoblotted with the TRPV1 antibody (Santa Cruz Biotechnology Inc. USA). A list of all antibodies and their dilutions used for the study are given in Table 2.

2.10. Quantitative RT-PCR analysis

Total RNA was isolated from EF tissues or 3T3-L1 cells using Trireagent (Sigma, USA) according to manufacturer's instructions. cDNA was synthesized using Quantitect reverse transcription kit (Qiagen, Valencia, CA) using Q5plex PCR system (Qiagen Valencia, CA). Real-time PCR was performed using QuantiTect SYBR green PCR kit on a Q5plex system. 18s was used as the reference gene. Amplification was performed in a 20 μL reaction volume according to manufacturer's instruction. Primer sequences for qPCR were used as per previously published research [11,12] and are provided in Table 3.

2.11. Chemicals and drugs

All chemicals and drugs were obtained from Sigma, USA. HFD was obtained from Research Diets Inc., NJ (D12492). Quantitative RT-PCR kits were obtained from Qiagen, USA.

2.12. Statistical analyses

All data are expressed as means ± S.E.M. Comparisons between groups were analyzed using one-way ANOVA and post hoc analyses were done using ANOVA or Student *t*-test, whenever appropriate. A P value < 0.05 was considered as statistically significant. Graphs from analyzed data were plotted using Microcal Origin 6.0 software.

3. Results

3.1. Feeding HFD causes obesity and suppresses TRPV1 but activation of TRPV1 by capsaicin promotes weight loss in the wild-type but not TRPV1$^{-/-}$ mice

Previously, we have shown in a mouse model of obesity that capsaicin feeding countered high-fat diet (HFD; 60% calories from FAT)-induced obesity and metabolic dysfunction without modifying energy intake [11,12]. To reconcile whether supplementation of capsaicin in the diet promotes weight loss in mice and causes browning of epididymal white adipose tissue (eWAT), we performed feeding experiments in wild-type and TRPV1$^{-/-}$ mice. As shown in Fig. 1A and B, both WT

Table 1
Food and water intake in WT and TRPV1$^{-/-}$ mice-fed HFD or HFD + capsaicin.

	WT		TRPV1$^{-/-}$	
	HFD	HFD + capsaicin (0.01%)	HFD	HFD + capsaicin (0.01%)
Food (g/day)	3.12 ± 0.23	3.14 ± 0.18	3.22 ± 0.38	3.29 ± 0.22
Energy intake (kCal/day)	16.35 ± 1.21	16.45 ± 0.94	16.87 ± 1.76	17.24 ± 1.12
Water (mL/day)	4.77 ± 0.88	4.81 ± 0.92	4.92 ± 1.02	4.88 ± 0.80

Table 2
Antibodies.
Sources of antibodies and dilutions used in the experiments are given below.

Antibodies and dilutions used	Source	Catalog No.
PPARα (1:500)	Novus Biologicals, USA	NB600-636
PPARγ (1:100)	Santa Cruz Biotechnology, Inc., USA	SC-7273
BMP8b (1:100)	Santa Cruz Biotechnology, Inc., USA	SC-13086
SIRT-1 (1:100)	Santa Cruz Biotechnology, Inc., USA	SC-28766
TRPV1 (1:100)	Santa Cruz Biotechnology, Inc., USA	SC-28759
Acetylated lysine (1:100 for IP)	Cell Signaling Inc., USA	9441
GAPDH (1:500)	Santa Cruz Biotechnology, Inc., USA	SC-365062
PGC-1α (1:1000)	Novus Biologicals, USA	NBP1-04676

Table 3
Primers for quantitative RT-PCR.
Primers (IDT, USA) that were used for RT-PCR experiments are given below.

Genes	Forward	Reverse
18s	5′-acc gca gct agg aat aat gga-3′	5′-gcc tca gtt ccg aaa acc a-3′
gapdh	5′-cgt gcc gcc tgg aga aac c-3′	5′-tgg aag agt ggg agt tgc tgt tg-3′
mtrpv1	5′-caa caa gaa ggg gct tac acc-3′	5′-tct gga gaa tgt agg cca aga c-3′
pparα	5′-gta cca cta cgg agt tca cgc at-3′	5′-cgc cga aag aag ccc tta c-3′
pparγ	5′-caa gaa tac caa agt gcg atc aa-3′	5′-gag cag ggt ctt ttc aga ata ata ag-3′
sirt-1	5′-tcg tgg aga cat ttt taa tca gg-3′	5′-gct tca tga tgg caa gtg g-3′
bmp8b	5′-tcc acc aac cac gcc act at-3′	5′-cag tag gca cac agc aca cct-3′

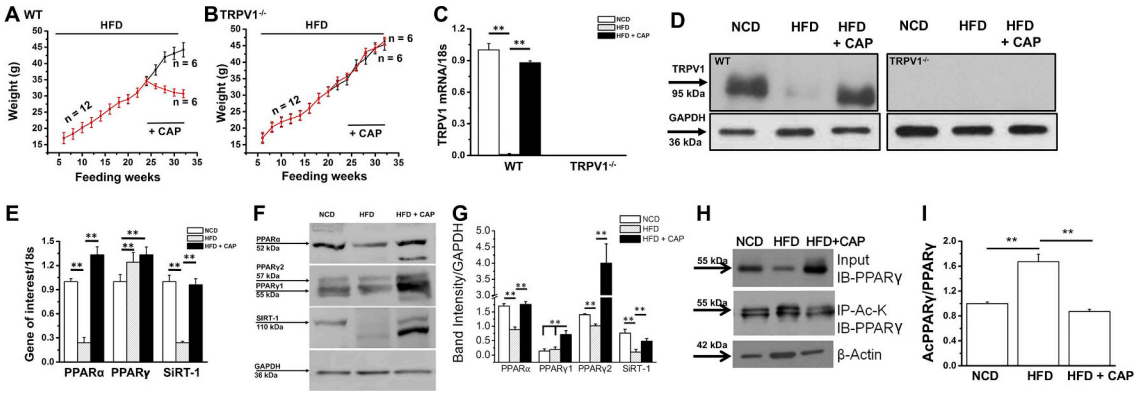

Fig. 1. Effect of CAP on HFD-induced weight gain, suppression of PPARs and SIRT-1 mRNA and acetylation of PPARγ in epididymal fat (EF) tissue. A and B. Time course of body weight changes in relation to weeks of feeding HFD (± CAP) in the WT and TRPV1$^{-/-}$ mice. Diet switch from HFD to HFD + CAP (0.01% in HFD) occurred on week 25. C. Mean TRPV1 mRNA ± S.E.M. normalized to 18s in epididymal fat from these mice. D. Immunoblot shows the expression of TRPV1 in the EF of NCD or HFD (± CAP)-fed WT and TRPV1$^{-/-}$ mice. E. Bar graphs represent the mean mRNA ± S.E.M. normalized to 18s for PPARα, PPARγ and SiRT-1 in epididymal fat from WT mice. F. Immunoblots show the expression of PPARα, PPARγ (1 and 2) and SiRT-1 in the EF of NCD or HFD (± CAP)-fed WT mice. G. Bar graphs show the mean band intensity ± S.E.M. (normalized to GAPDH) for the expression of PPARα,γ (1 and 2) and SiRT-1. H. EF samples of NCD or HFD (± CAP)-fed WT mice immunoblotted for PPARγ and immunoprecipitated with acetylated lysine antibody (Ac-K). I. The mean ratio of acetylated PPARγ to total PPARγ ± S.E.M. ** represents statistical significance for $P < 0.01$ for 4 independent experiments.

and TRPV1$^{-/-}$ mice gained weight upon HFD feeding and supplementation of capsaicin in HFD (from weeks 25 to 32) inhibited weight gain only in the WT but not in TRPV1$^{-/-}$ mice. Capsaicin feeding did not alter the energy and water intake in these mice (Table 1). Also, capsaicin feeding restored TRPV1 mRNA and protein in the eWAT of WT mice (Fig. 1C and D). Supplementation of capsaicin reversed the inhibitory effect of HFD on the mRNA levels and protein expression of PPARα and SiRT-1 (Fig. 1E, F and G).

3.2. TRPV1 activation by capsaicin increases the deacetylation of PPARγ in the epididymal fat (EF)

PPARγ plays an important role in adipogenesis and its deacetylation by SiRT-1 stabilizes it and promotes its interaction with PRDM-16, a regulator of browning program in WAT. Previous studies have shown that PPARγ deacetylation triggers browning of inguinal white adipose tissue. Capsaicin has also been shown previously to promote browning of inguinal adipose tissues. However, whether capsaicin causes browning of EF has not been studied before. Therefore, we analyzed the expression and acetylated levels of PPARγ in the EF isolated from WT mice that received HFD or HFD + capsaicin. As shown in Fig. 1H and I, PPARγ acetylation was enhanced by HFD in eWAT and capsaicin reversed this.

3.3. Characterization of TRPV1 in 3T3-L1 cells

We evaluated the effect of overexpression of TRPV1 in 3T3-L1 cells to study the alterations in thermogenic genes and proteins. Overexpression studies have potential advantages in identifying targets as well as phenotypes [16]. First, we measured the endogenous TRPV1 mRNA levels in 3T3-L1 cells by quantitative real-time PCR (qPCR) method. We used HEK 293 cells overexpressing TRPV1 as a control for this experiment. We overexpressed TRPV1 in 3T3-L1 cells by transfecting the cells with TRPV1 cDNA as described under the methods section of the manuscript. Overexpression of TRPV1 enhanced TRPV1 mRNA and protein in the 3T3-L1 cells. These results are summarized in Fig. 2A, B and C. We used TRPV1 overexpressing 3T3-L1 cells (designated as 3T3-L1^{TRPV1}) for further experiments.

Next, we stimulated 3T3-L1^{TRPV1} cells with capsaicin in the absence (Fig. 2B) and presence (Fig. 2D and E) of a TRPV1 antagonist. Capsazepine (TRPV1 antagonist) pretreatment (30 min 10 μM) prevented capsaicin-stimulated Ca^{2+} influx in these cells.

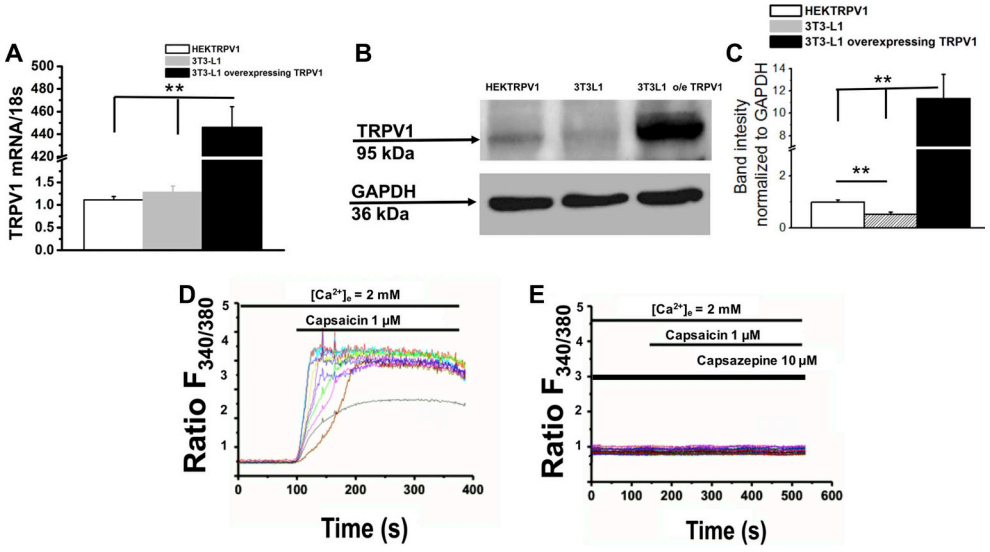

Fig. 2. TRPV1 expression and activity in 3T3-L1 cells. A. TRPV1 mRNA normalized to 18s in HEKTRPV1, 3T3-L1, and 3T3-L1^{TRPV1} cells. B. Immunoblot shows the expression of TRPV1 in HEKTRPV1, 3T3-L1, and 3T3-L1^{TRPV1} cells. GAPDH is a loading control C. Bar graphs represent mean band intensity for TRPV1 expression in these cells normalized to GAPDH. CAP (1 μM)-stimulated Ca^{2+} influx in control (D) and capsazepine (CPZ; 10 μM; TRPV1 antagonist) pretreated (E) 3T3-L1^{TRPV1} cells. Cells were preincubated with CPZ for 30 min prior to experiment and CPZ was present continuously as indicated in the figure. ** represents statistical significance for $P < 0.01$ for 8 independent experiments. Colors represent the response from several cells seeded on the same coverslip.

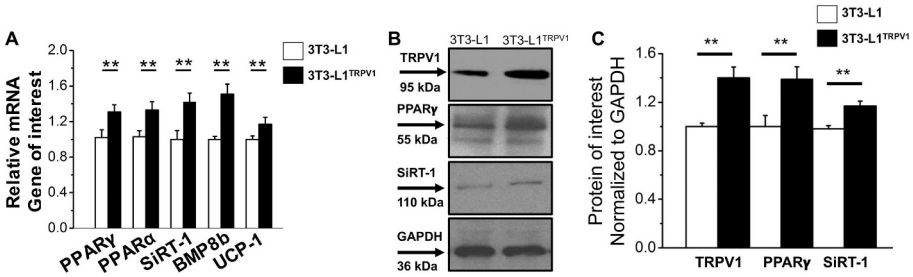

Fig. 3. Overexpression of TRPV1 increases the expression of thermogenic genes in 3T3-L1 cells. A. Bar graphs represent the mean mRNA ± S.E.M. normalized to 18s for PPARγ, PPARα, SiRT-1, BMP8b, and UCP-1 in control (open columns) and TRPV1 overexpressing (shaded columns) 3T3-L1^{TRPV1} cells. B. Immunoblots show the expression of TRPV1, PPARγ, and SiRT-1 in these cells. C. Bar graphs represent the mean protein intensity ± S.E.M. normalized to GAPDH. ** represents statistical significance for $P < 0.05$ for 6 independent experiments.

3.4. TRPV1 overexpression increases mRNA levels and expression of PPARγ, PPARα, SiRT-1, BMP8b, and UCP-1 in 3T3-L1 cells

Next, we analyzed the expression of adipogenic and thermogenic genes and proteins in 3T3-L1 cells (Fig. 3) by quantitative RT-PCR technique and by western blotting. Overexpression of TRPV1 significantly increased the mRNA levels (Fig. 3A) and expression of PPARα, PPARγ. SiRT-1, BMP8b, and UCP-1 (Fig. 3B). The quantification of mean band intensities ± S.E.M. normalized to GAPDH for experiments performed in triplicates is given in Fig. 3C.

3.5. Differentiation of 3T3-L1^{TRPV1} cells progressively increases lipid accumulation but decreases TRPV1 expression and suppresses its activity

Next, we differentiated 3T3-L1^{TRPV1} cells as per the method described under materials and methods section. We followed an eight-day differentiation protocol for this. We analyzed the accumulation of lipid droplets in undifferentiated and 4 or 8 days differentiated 3T3-L1^{TRPV1} cells by oil red O staining method. Alternatively, we analyzed the lipid content in these cells by a spectroscopic method. We also measured the TRPV1 mRNA levels and analyzed capsaicin-stimulated Ca^{2+} influx in these cells. We determined the expression of the TRPV1 protein in undifferentiated and differentiated (day 8) 3T3-L1^{TRPV1} cell lysate by immunoprecipitation. Differentiation process increased lipid accumulation in 3T3-L1^{TRPV1} as shown by the oil red O staining of these cells on day 4 and 8 of differentiation (Supplemental Fig. 1A, B and C). Consistently, the absorbance of lipids also increased as illustrated in Fig. 3D. However, the levels of TRPV1 mRNA and activity of TRPV1 decreased upon 3T3-L1^{TRPV1} differentiation. As shown in Supplemental Fig. 1E, F and G, with the increase in lipid accumulation, both the mRNA levels and activity of TRPV1 are decreased in 3T3-L1^{TRPV1} cells. Western blot for TRPV1 protein in undifferentiated and differentiated (day 8; Supplemental Fig. 1H) 3T3-L1^{TRPV1} cells confirms that lipid accumulation has a suppressive effect on TRPV1 expression. This is consistent with previous reports that suggest that increased lipid accumulation is associated with a concomitant reduction in both expression and activity of TRPV1 [11,12]. Also, a previous study suggests that with an increase in visceral fat, a reduction in the expression of TRPV1 was observed in humans [10].

3.6. Troglitazone enhances the expression and activity of TRPV1 in 3T3-L1 cells

Published research suggests that TRPV1 activation by capsaicin enhances the expression of PPARγ in adipose tissue. To determine whether PPARγ activation alters TRPV1, we evaluated the effect of the acute application of Trog (10 μM) on 3T3-L1^{TRPV1} cells. Surprisingly, acute Trog treatment activated a robust Ca^{2+} influx into 3T3-L1^{TRPV1} cells, which was inhibited by pretreatment with capsazepine (CPZ; 10 μM) in these cells (Fig. 4A). Since the mRNA levels and expression of PPARα were increased in 3T3-L1^{TRPV1}, we evaluated the effect of PPARα agonist (Clofibrate, CLO) on TRPV1 activity. We treated 3T3-L1^{TRPV1} cells with CLO (10 μM) and measured the intracellular Ca^{2+} signal. As shown in Fig. 4C, CLO failed to activate TRPV1. The summary of mean changes in Trog (± capsazepine) and CLO stimulated Ca^{2+} influx ± S.E.M. in 3T3-L1^{TRPV1} cells is shown in Fig. 4D. In order to test whether Trog can stimulate a Ca^{2+} influx in cells that lack TRPV1, we treated control HEK293 cells, which do not express TRPV1 endogenously. As shown in Fig. 4E, Trog did not induce Ca^{2+} influx in these cells. However, in HEKTRPV1 cells, both Trog and another TZD derivative, Rosiglitazone (Rosi; 10 μM), induced a Ca^{2+} influx, which was inhibited by CPZ (Supplemental Fig. 2). However, as illustrated in Supplemental Fig. 2C and F, the effect of Rosi was slower and not as robust as Trog. The mean change in fluorescence ratio (F340/380) following Trog was 1.6 ± 0.28 while that with Rosi was 0.4 ± 0.12. However, pretreatment with CPZ inhibited the effects of Trog and Rosi (Supplemental Fig. 2B and E).

Next, we evaluated the effect of Trog on epididymal adipocytes isolated from NCD-fed WT and TRPV1$^{-/-}$ mice. As illustrated in Supplemental Fig. 3, acute Trog treatment initiated Ca^{2+} influx in the epididymal adipocytes of WT but not TRPV1$^{-/-}$ mice.

3.7. Differentiation process increases c/EBPα and PPARγ while decreases PPARα, SiRT-1, and BMP8b in 3T3-L1^{TRPV1} cells

Adipogenesis is a cell differentiation process by which pre-adipocytes are converted in to mature adipocytes. PPARγ and c/EPBα are critical regulators of adipogenesis [17]. Therefore, we measured the expression of these genes and other thermogenic genes in undifferentiated and differentiated 3T3-L1^{TRPV1} cells. As shown in

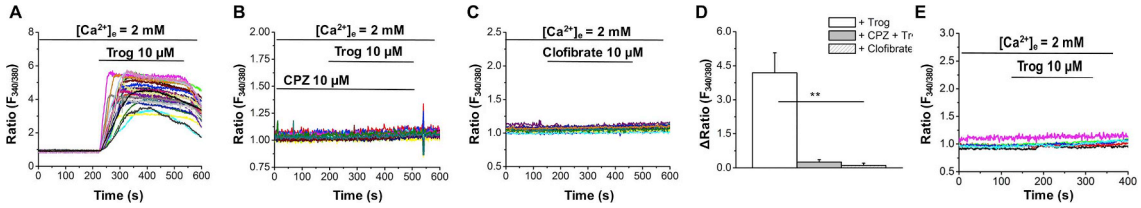

Fig. 4. Troglitazone directly activates TRPV1. Time courses of Trog (10 μM)-stimulated Ca^{2+} influx in control (A) and capsazepine (CPZ; 10 μM; TRPV1 antagonist) pretreated (B) 3T3-L1^{TRPV1} cells. C. Time courses of Clofibrate (CLO; 10 μM)-stimulated Ca^{2+} influx in 3T3-L1^{TRPV1} cells. D. Mean fluorescence change ± S.E.M. following Trog treatment (± CPZ) or CLO in 3T3-L1^{TRPV1} cells (n = 88–132 cells/condition). E. Representative traces showing the time courses of Trog (10 μM)-stimulated Ca^{2+} influx in control HEK293 cells (n = 36). ** represents statistical significance for $P < 0.01$. Colors represent the response from several cells seeded on the same coverslip.

Supplemental Fig. 4A, on day 8 of differentiation, the mRNA levels of c/EBPα and PPARγ were increased, while that of PPARα, SiRT-1, and BMP8b were decreased compared with the undifferentiated 3T3-L1^{TRPV1} cell. We could not detect the expression of mitochondrial uncoupling protein 1 (UCP-1) in both undifferentiated and differentiated. This is consistent with a previous study which describes the lack of endogenous UCP-1 in 3T3-L1 cells [18].

3.8. Effect of Troglitazone on TRPV1 and genes of adipogenesis and thermogenesis in undifferentiated and differentiated 3T3-L1^{TRPV1} cells

Trog is a PPARγ agonist, which enhances insulin sensitivity [19]. Recent studies show that PPARγ is required for inducing browning of WAT [5,20]. So, we evaluated the effect of Trog treatment on the expression of adipogenic and thermogenic genes in undifferentiated and differentiated (8 day) 3T3-L1^{TRPV1} cells. 3T3-L1^{TRPV1} cells were treated with Trog (10 μM) for 12 h prior to quantitative RT-PCR (qPCR) measurements. As described in Supplemental Fig. 4B, Trog treatment significantly increased the mRNA levels of TRPV1, c/EBPα, PPARγ, SiRT-1, and BMP8b only in the undifferentiated cells. However, Trog increased the mRNA levels of c/EBPα and PPARγ in the differentiated cells. Trog treatment did not alter the expression of PPARα mRNA levels under both conditions.

3.9. Troglitazone enhances the expression of TRPV1 and thermogenic proteins in 3T3-L1 cells and TRPV1 inhibition by capsazepine prevents this

Since Trog activates TRPV1 in vitro, we evaluated the effect of Trog treatment on the expression of TRPV1 and thermogenic proteins in 3T3-L1 and 3T3-L1^{TRPV1} cells. These cells were treated with Trog (10 μM) for 12 h prior to quantitative RT-PCR (qPCR) measurements. As illustrated in Fig. 5, Trog treatment significantly increased the expression of TRPV1, PPARα, BMP8b, PGC-1α, PPARγ, and SiRT-1 in these cells. Also, we evaluated the effect of capsaicin treatment in vitro on the expression of thermogenic proteins in 3T3-L1^{TRPV1} cells. For this, we treated cells with either vehicle or capsaicin (1 μM) for 90 min and then analyzed the expression levels of TRPV1, PPARα, BMP8b, PGC-1α, PPARγ, and SiRT-1. As shown in Fig. 5D and E, acute capsaicin treatment significantly elevated the expression of these proteins. These data together suggest that activation of TRPV1 by Trog or capsaicin has a similar enhancing effect on the expression of thermogenic proteins.

Next, we analyzed whether inhibition of TRPV1 will reverse the stimulatory effect of Trog on thermogenic protein expression in 3T3-L1^{TRPV1} cells. For this, we pretreated a sub-group of these cells with capsazepine (CPZ; 10 μM) and then stimulated with Trog (10 μM; 90 min) and analyzed the expression of TRPV1, PPARα, BMP8b, PGC-1α, PPARγ and SiRT-1 by immunoblotting. As shown in Fig. 6, CPZ treatment significantly downregulated the stimulatory effect of Trog on the expression of these proteins.

3.10. Trog induces the deacetylation of PPARγ by activating TRPV1 in 3T3-L1 cells

Deacetylation of PPARγ by SiRT-1 has been recognized as a browning mechanism of WAT [5]. Previous research has shown that thiazolidinedione treatment caused deacetylation of PPARγ [5], stabilized PRDM-16 [20] to stimulate the browning of WAT. Further, the deacetylation of PPARγ by its agonists has been shown to promote their benefits to treat metabolic diseases [21]. Since TRPV1 activation by capsaicin enhanced PPARγ deacetylation and browning of WAT [11], we hypothesized that Trog will also induce PPARγ deacetylation via TRPV1. First, we analyzed the expression of PPARγ in Trog treated control and TRPV1 overexpressing cells. Trog increased the expression of PPARγ under both conditions (Fig. 7A and B). To evaluate whether Trog stimulates PPARγ deacetylation, we treated 3T3-L1^{TRPV1} cells with capsaicin (1 μM for 12 h) or Trog (10 μM for 12 h) in the absence or presence of capsazepine (10 μM, treated 90 min prior to capsaicin or Trog treatment) at 37 °C. We then performed a coimmunoprecipitation

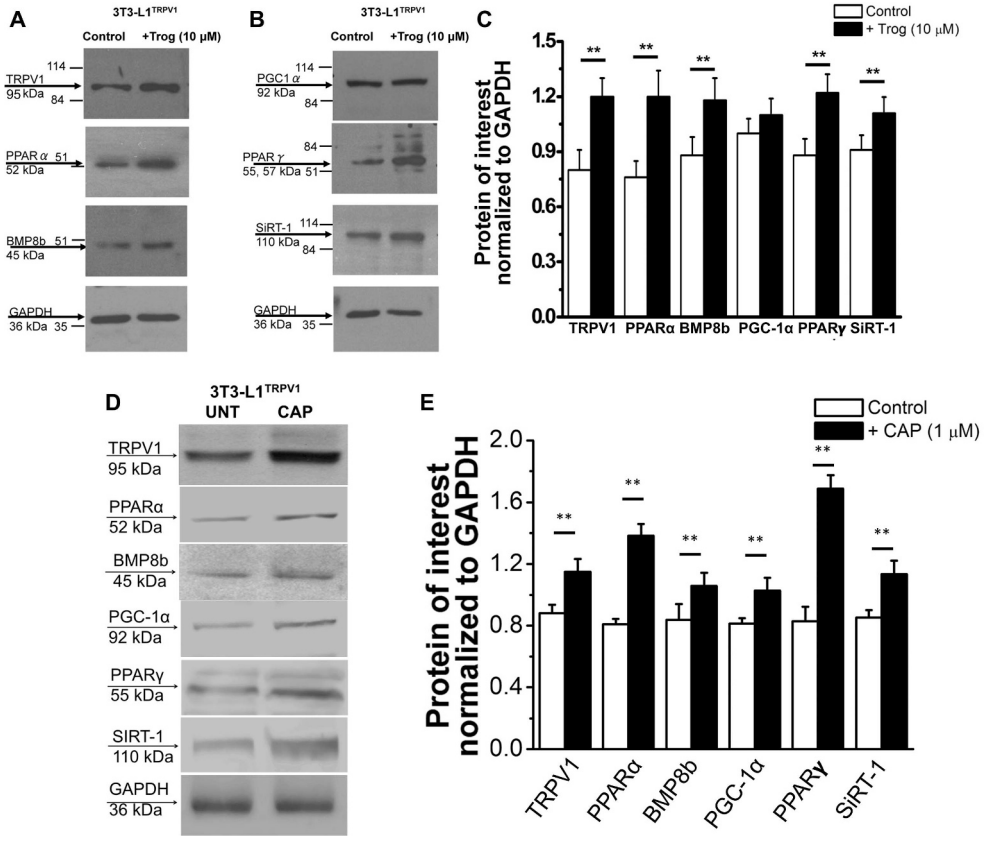

Fig. 5. Effect of acute Trog treatment on the expression of TRPV1 and thermogenic proteins. A and B. Representative western blots for TRPV1, PPARα, BMP8b, PGC-1α, PPARγ, and SiRT-1 in the control and Trog (10 μM; 90 min) treated 3T3-L1^{TRPV1} cells. D. Representative western blots for TRPV1, PPARα, BMP8b, PGC-1α, PPARγ, and SiRT-1 in the control and capsaicin (CAP; 1 μM; 90 min) treated 3T3-L1^{TRPV1} cells. GAPDH was a loading control. C and E. Mean band intensities of these proteins ± S.E.M. normalized to GAPDH in Trog or capsaicin-treated cells. ** represents statistical significance for $P < 0.01$ for $n = 3$ experiments/condition.

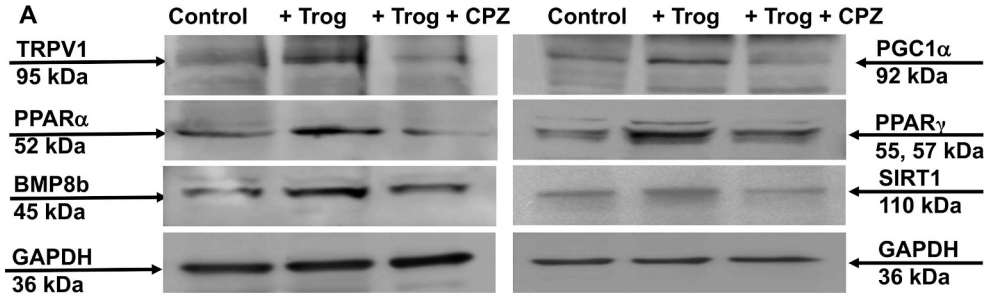

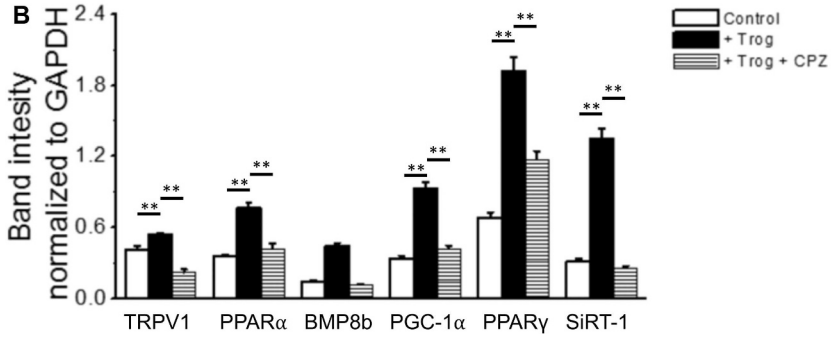

Fig. 6. Troglitazone enhances the expression of thermogenic proteins in 3T3-L1^{TRPV1} cells and inhibition of TRPV1 prevents this. A. Representative blots show the expression of TRPV1, PPARα, BMP8b, PGC-1α, PPARγ and SiRT-1 in control, Trog (10 μM for 90 min) and Trog + CPZ (10 μM for 90 min) treated 3T3-L1^{TRPV1} cells. GAPDH is a loading control. B. Bar graphs show the mean protein expression ± S.E.M. ($n = 3$) for these proteins. ** Statistical significance for $P < 0.05$.

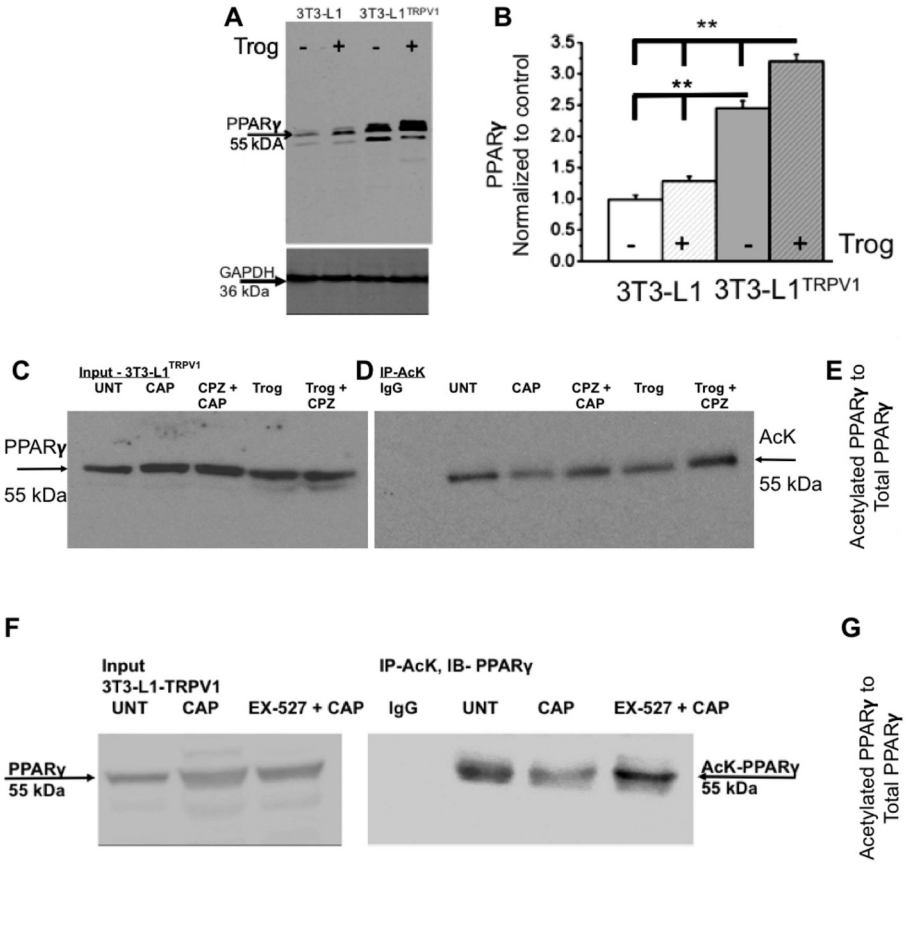

Fig. 7. Capsaicin (CAP) and Trog enhance PPARγ deacetylation and inhibition of TRPV1 prevents this. A. Western blot showing the expression of PPARγ in Trog treated (10 μM; 12 h) control and TRPV1 overexpressing 3T3-L1 cells. B. Mean band intensities of PPARγ normalized to GAPDH. C. Representative immunoblots ($n = 3$) showing the expression of PPARγ in the input of CAP (± capsazepine, CPZ) or Trog (± CPZ) treated 3T3-L1^{TRPV1} cells. D. Acetylated PPARγ in these cells following immunoprecipitation with AcK antibody. E. The ratio of acetylated PPARγ to total PPARγ. F. Representative immunoblots ($n = 3$) showing the expression of PPARγ and acetylated PPARγ in the input of control and CAP (± EX527; SiRT-1 inhibitor; 10 μM; 1 h pretreatment) in 3T3-L1^{TRPV1} cells. G. The ratio of acetylated PPARγ to total PPARγ.

experiment to immunoprecipitate PPARγ using acetylated lysine (AcK) antibody (Fig. 7C and D). Experiments were performed in triplicates and the ratio of band intensities of acetylated PPARγ to total PPARγ was calculated and represented in Fig. 7E.

In order to determine whether TRPV1 activation promotes PPARγ deacetylation by activating SiRT-1, we pretreated cells with a SiRT-1 inhibitor (EX527; 10 μM; 1 h) and then stimulated with capsaicin. As illustrated in Fig. 7F and G, Ex527 increased the levels of acetylated PPARγ, thus preventing the effect of capsaicin on PPARγ deacetylation via SiRT-1.

4. Discussion

Strategies to stimulate the conversion of energy-storing white fat to energy expending brown fat-like phenotype (also referred to as beige fat) have received significant attention in recent years [22–25]. Predominately, the activation of SiRT-1, an NAD^+-dependent deacetylase, and its subsequent deacetylation of PPARγ, PRDM-16, and their stabilization to promote thermogenic program have been regarded as mechanisms underlying the browning of WAT [5,11,20,26]. Consistently, several studies have demonstrated that the deacetylation of PPARγ is a marker for browning of WAT [5,11,27]. Specifically, research work demonstrating the novel role of thiazolidinedione (TZD) derivatives in SiRT-1-dependent deacetylation of PPARγ presents a new mechanism for the benefits of these molecules despite any adverse reactions associated with their use [21].

Recently, TRPV1 has been identified as a novel partner in this browning phenomenon [11,28]. Published data suggest that activation of TRPV1 prevents diet-induced obesity by causing the browning of WAT via SiRT-1-dependent deacetylation of PPARγ [12]. The use of capsaicin or its non-pungent analogs in clinical trials has been shown to be beneficial [29-37]. However, the precise mechanism(s) by which TRPV1 activation enhances energy expenditure and combats nutrient overload-induced metabolic dysfunction remains unclear. Pertinent to the role of TRPV1 in the browning of WAT, the results presented in this work suggest a cross-talk between PPARγ and TRPV1 signaling since TRPV1 activation enhanced the expression and deacetylation of PPARγ in epididymal fat (in vivo) as well as 3T3-L1^{TRPV1} cells in vitro. Moreover, our results illustrating the enhancement of adipogenic and thermogenic protein expression in TRPV1 overexpressing 3T3-L1 cells indicates a critical role of TRPV1 in adipogenic and thermogenic processes. These results validate that TRPV1 is a potential candidate for inducing browning of WAT.

This study has discovered an interesting cross-talk between TZD and TRPV1 and shows a direct activating effect of TRPV1 by TZD derivatives. Recently, PPARγ agonists have been shown to cause browning of white adipocytes [5,20,38,39] by stabilizing PPARγ and PRDM-16, a gene responsible for this molecular switch. Since TRPV1 activation caused browning of white adipose tissue, TZDs may trigger browning program in 3T3-L1 cells TRPV1 activation. The ability of Trog and Rosi to activate TRPV1 as well as enhance PPARγ rises an important question – whether these compounds mediate this effect directly or via PPARγ. However, in control HEK293 cells that lack TRPV1 endogenously, Trog failed to stimulate a Ca^{2+} influx. These data suggest that Trog presumably mediates its effect directly on TRPV1 and not via PPARγ activation. Also, the induction of Ca^{2+} influx by Trog was spontaneous in 3T3-L1^{TRPV1} cells as there was no time delay between the application of Trog and the influx of Ca^{2+}. However, the effect of Rosi was lower than Trog. One reason for this could be the difference in the structure of these compounds. Further in vitro studies and molecular docking analyses are required to address this. Nevertheless, our data demonstrate that TRPV1 is activated by TZD, which will have a clinical significance since TZDs are used as insulin sensitizing agents as they activate PPARγ. Published literature suggests that activation of TRPV1 also improves insulin sensitivity and promotes better glucose handling in rodents. Therefore, it is reasonable to speculate a permissive role of TRPV1 activation in the insulin-sensitizing effects of TZDs. However, whether TRPV1 activation modulates the transcriptional activity of PPARγ still remains to be determined. Nonetheless, capsaicin or Trog treatment not only enhanced the expression of PPARγ in 3T3-L1^{TRPV1} cells but also decreased its acetylated levels in 3T3-L1^{TRPV1} cells. Further, this effect of capsaicin or Trog is reversed by TRPV1 inhibition. Moreover, inhibition of SiRT-1 by EX527 prevents the deacetylation of PPARγ by capsaicin. These observations raise important questions on the ability of TRPV1 activation on the transcriptional activity of PPARγ. Future studies are warranted to clarify this.

This study presents an interesting observation that TRPV1 expression and activity were suppressed in differentiated 3T3-L1^{TRPV1} cells. We observed a progressive loss of TRPV1 in these cells as differentiation progressed. Also, Trog failed to enhance TRPV1 and thermogenic BMP8b and SiRT-1 in differentiated 3T3-L1 cells. We performed experiments to overexpress TRPV1 in these cells but the transfection efficiency was very low. These data indicate that accumulation of fat (lipid) during the differentiation process suppresses TRPV1. This is consistent with a previous report, which suggests the suppressive effect of differentiation on TRPV1 in 3T3-L1 cells [28]. Further, the suppression of BMP8b and SiRT-1 in the differentiated cells also suggests that lipid accumulation has a profound inhibitory effect on thermogenic genes. However, the molecular mechanisms by which lipid accumulation downregulates TRPV1 and other thermogenic genes still remain to be determined.

Collectively, this research sheds new light on the activating role of TZD on TRPV1 and in the regulation of adipogenic and thermogenic protein expression in 3T3-L1^{TRPV1} cells. Based on this, it is reasonable to speculate the existence of an unexplored direct or an indirect crosstalk between TRPV1 and PPARγ, which could be important for the browning of WAT. If TZD can activate TRPV1 to enhance the browning of WAT, will TRPV1 play a direct role in insulin sensitization mechanisms of TZD? This is significant since capsaicin has been shown previously to enhance insulin sensitivity and improve glucose tolerance [40-45] in mice. Until now, such a beneficial effect of TRPV1 activation is often considered as secondary to its anti-obesity action. The direct effect of TZD to activate TRPV1 and enhance PPARγ deacetylation via TRPV1-dependent pathway indicates a more direct role of TRPV1 activation in glucose homeostasis. Further, in vivo studies are required to decipher this and evaluate the role of TRPV1 in the beneficial and adverse effects of TZD. Nevertheless, the data presented here demonstrate the potential of TRPV1 as an attractive target for ameliorating metabolic dysfunctions.

Supplementary data to this article can be found online at https://doi.org/10.1016/j.bbadis.2018.11.004.

Transparency document

The Transparency document associated with this article can be found, in online version.

Acknowledgment

The work was supported by a Thematic Research Grant from the National Institute of General Medical Sciences of the National Institutes of Health under Award Number 8P20GM103432-12, and University of Wyoming Faculty Grant in Aid to BT.

Conflict of interest

None. The authors indicate that there is no conflict of interests to declare.

Author contribution

VK – Performed experiments.

PB – Performed experiments, analyzed results, wrote the manuscript.

BT – Designed experiments, performed experiments, analyzed results and wrote the manuscript.

References

[1] S. Kersten, B. Desvergne, W. Wahli, Roles of PPARs in health and disease, Nature 405 (2000) 421–424.
[2] L. Chen, G. Yang, PPARs integrate the mammalian clock and energy metabolism, PPAR Res. 2014 (2014) 653017.
[3] K. Farrajota, S. Cheng, J. Martel-Pelletier, H. Afif, J.P. Pelletier, X. Li, P. Ranger, H. Fahmi, Inhibition of interleukin-1beta-induced cyclooxygenase 2 expression in human synovial fibroblasts by 15-deoxy-Delta12,14-prostaglandin J2 through a histone deacetylase-independent mechanism, Arthritis Rheum. 52 (2005) 94–104.
[4] L. Tian, C. Wang, F.K. Hagen, M. Gormley, S. Addya, R. Soccio, M.C. Casimiro, J. Zhou, M.J. Powell, P. Xu, H. Deng, A.A. Sauve, R.G. Pestell, Acetylation-defective mutant of Ppargamma is associated with decreased lipid synthesis in breast cancer cells, Oncotarget 5 (2014) 7303–7315.
[5] L. Qiang, L. Wang, N. Kon, W. Zhao, S. Lee, Y. Zhang, M. Rosenbaum, Y. Zhao, W. Gu, S.R. Farmer, D. Accili, Brown remodeling of white adipose tissue by SirT1-dependent deacetylation of Ppargamma, Cell 150 (2012) 620–632.
[6] B. Cannon, J. Nedergaard, Brown adipose tissue: function and physiological significance, Physiol. Rev. 84 (2004) 277–359.
[7] M.G. Kolonin, How brown is brown fat that we can see? Adipocytes 3 (2014) 155–159.
[8] C. Montell, The TRP superfamily of cation channels, Sci. STKE 2005 (2005) re3.
[9] J. Vriens, G. Appendino, B. Nilius, Pharmacology of vanilloid transient receptor potential cation channels, Mol. Pharmacol. 75 (2009) 1262–1279.
[10] L.L. Zhang, D. Yan Liu, L.Q. Ma, Z.D. Luo, T.B. Cao, J. Zhong, Z.C. Yan, L.J. Wang, Z.G. Zhao, S.J. Zhu, M. Schrader, F. Thilo, Z.M. Zhu, M. Tepel, Activation of transient receptor potential vanilloid type-1 channel prevents adipogenesis and obesity, Circ. Res. 100 (2007) 1063–1070.
[11] P. Baskaran, V. Krishnan, J. Ren, B. Thyagarajan, Capsaicin induces browning of white adipose tissue and counters obesity by activating TRPV1 channel-dependent mechanisms, Br. J. Pharmacol. 173 (2016) 2369–2389.
[12] P. Baskaran, V. Krishnan, K. Fettel, P. Gao, Z. Zhu, J. Ren, B. Thyagarajan, TRPV1 activation counters diet-induced obesity through sirtuin-1 activation and PRDM-16 deacetylation in brown adipose tissue, Int. J. Obes. 41 (2017) 739–749.
[13] M.J. Curtis, R.A. Bond, D. Spina, A. Ahluwalia, S.P. Alexander, M.A. Giembycz, A. Gilchrist, D. Hoyer, P.A. Insel, A.A. Izzo, A.J. Lawrence, D.J. MacEwan, L.D. Moon, S. Wonnacott, A.H. Weston, J.C. McGrath, Experimental design and analysis and their reporting: new guidance for publication in BJP, Br. J. Pharmacol. 172 (2015) 3461–3471.
[14] G.L. Humason, Animal Tissue Techniques, Freeman, San Francisco, CA, 1972.
[15] V. Lukacs, B. Thyagarajan, P. Varnai, A. Balla, T. Balla, T. Rohacs, Dual regulation of TRPV1 by phosphoinositides, J. Neurosci. 27 (2007) 7070–7080.
[16] G. Prelich, Gene overexpression: uses, mechanisms, and interpretation, Genetics 190 (2012) 841–854.
[17] E.D. Rosen, C.H. Hsu, X. Wang, S. Sakai, M.W. Freeman, F.J. Gonzalez, B.M. Spiegelman, C/EBPalpha induces adipogenesis through PPARgamma: a unified pathway, Genes Dev. 16 (2002) 22–26.
[18] H. Asano, Y. Kanamori, S. Higurashi, T. Nara, K. Kato, T. Matsui, M. Funaba, Induction of beige-like adipocytes in 3T3-L1 cells, J. Vet. Med. Sci. 76 (2014) 57–64.
[19] W.C. Knowler, R.F. Hamman, S.L. Edelstein, E. Barrett-Connor, D.A. Ehrmann, E.A. Walker, S.E. Fowler, D.M. Nathan, S.E. Kahn, G. Diabetes Prevention, Program research, prevention of type 2 diabetes with troglitazone in the diabetes prevention program, Diabetes 54 (2005) 1150–1156.
[20] H. Ohno, K. Shinoda, B.M. Spiegelman, S. Kajimura, PPARgamma agonists induce a white-to-brown fat conversion through stabilization of PRDM16 protein, Cell Metab. 15 (2012) 395–404.
[21] M.J. Kraakman, Q. Liu, J. Postigo-Fernandez, R. Ji, N. Kon, D. Larrea, M. Namwanje, L. Fan, M. Chan, E. Area-Gomez, W. Fu, R.J. Creusot, L. Qiang, PPARgamma deacetylation dissociates thiazolidinedione's metabolic benefits from its adverse effects, J. Clin. Invest. 128 (2018) 2600–2612.
[22] A. Fenzl, F.W. Kiefer, Brown adipose tissue and thermogenesis, Horm. Mol. Biol. Clin. Invest. 19 (2014) 25–37.
[23] C. Forest, N. Joffin, A.M. Jaubert, P. Noirez, What induces watts in WAT? Adipocytes 5 (2016) 136–152.
[24] A. Nakhuda, A.R. Josse, V. Gburcik, H. Crossland, F. Raymond, S. Metairon, L. Good, P.J. Atherton, S.M. Phillips, J.A. Timmons, Biomarkers of browning of white adipose tissue and their regulation during exercise- and diet-induced weight loss, Am. J. Clin. Nutr. 104 (2016) 557–565.
[25] B. Thyagarajan, M.T. Foster, Beiging of white adipose tissue as a therapeutic strategy for weight loss in humans, Horm. Mol. Biol. Clin. Invest. 31 (2017).
[26] L. Wang, R. Teng, L. Di, H. Rogers, H. Wu, J.B. Kopp, C.T. Noguchi, PPARalpha and Sirt1 mediate erythropoietin action in increasing metabolic activity and browning of white adipocytes to protect against obesity and metabolic disorders, Diabetes 62 (2013) 4122–4131.
[27] H. Wang, L. Liu, J.Z. Lin, T.R. Aprahamian, S.R. Farmer, Browning of white adipose tissue with roscovitine induces a distinct population of UCP1+ adipocytes, Cell Metab. 24 (2016) 835–847.
[28] R.K. Baboota, D.P. Singh, S.M. Sarma, J. Kaur, R. Sandhir, R.K. Boparai, K.K. Kondepudi, M. Bishnoi, Capsaicin induces "brite" phenotype in differentiating 3T3-L1 preadipocytes, PLoS One 9 (2014) e103093.
[29] B. Faraut, B. Giannesini, V. Matarazzo, Y. Le Fur, G. Rougon, P.J. Cozzone, D. Bendahan, Capsiate administration results in an uncoupling protein-3 down-regulation, an enhanced muscle oxidative capacity and a decreased abdominal fat content in vivo, Int. J. Obes. 33 (2009) 1348–1355.
[30] B. Faraut, B. Giannesini, V. Matarazzo, T. Marqueste, C. Dalmasso, G. Rougon, P.J. Cozzone, D. Bendahan, Downregulation of uncoupling protein-3 in vivo is linked to changes in muscle mitochondrial energy metabolism as a result of capsiate administration, Am. J. Physiol. Endocrinol. Metab. 292 (2007) E1474–E1482.
[31] S. Haramizu, F. Kawabata, Y. Masuda, K. Ohnuki, T. Watanabe, S. Yazawa, T. Fushiki, Capsinoids, non-pungent capsaicin analogs, reduce body fat accumulation without weight rebound unlike dietary restriction in mice, Biosci. Biotechnol. Biochem. 75 (2011) 95–99.
[32] S. Haramizu, F. Kawabata, K. Ohnuki, N. Inoue, T. Watanabe, S. Yazawa, T. Fushiki, Capsiate, a non-pungent capsaicin analog, reduces body fat without weight rebound like swimming exercise in mice, Biomed. Res. 32 (2011) 279–284.
[33] M.J. Ludy, G.E. Moore, R.D. Mattes, The effects of capsaicin and capsiate on energy balance: critical review and meta-analyses of studies in humans, Chem. Senses 37 (2012) 103–121.
[34] Y. Masuda, S. Haramizu, K. Oki, K. Ohnuki, T. Watanabe, S. Yazawa, T. Kawada, S. Hashizume, T. Fushiki, Upregulation of uncoupling proteins by oral administration of capsiate, a nonpungent capsaicin analog, J. Appl. Physiol. 95 (2003) 2408–2415.
[35] K. Ohyama, Y. Nogusa, K. Shinoda, K. Suzuki, M. Bannai, S. Kajimura, A synergistic antiobesity effect by a combination of capsinoids and cold temperature through promoting beige adipocyte biogenesis, Diabetes 65 (2016) 1410–1423.
[36] K. Ohyama, K. Suzuki, Dihydrocapsiate improved age-associated impairments in mice by increasing energy expenditure, Am. J. Physiol. Endocrinol. Metab. 313 (2017) E586–E597.
[37] C. Zsiboras, R. Matics, P. Hegyi, M. Balasko, E. Petervari, I. Szabo, P. Sarlos, A. Miko, J. Tenk, I. Rostas, D. Pecsi, A. Garami, Z. Rumbus, O. Huszar, M. Solymar, Capsaicin and capsiate could be appropriate agents for treatment of obesity: a meta-analysis of human studies, Crit. Rev. Food Sci. Nutr. 58 (2018) 1419–1427.
[38] F.G. Zadegan, K. Ghaedi, S.M. Kalantar, M. Peymani, M.S. Hashemi, H. Baharvand, M.H. Nasr-Esfahani, Cardiac differentiation of mouse embryonic stem cells is influenced by a PPAR gamma/PGC-1alpha-FNDC5 pathway during the stage of cardiac precursor cell formation, Eur. J. Cell Biol. 94 (2015) 257–266.
[39] A. Loft, I. Forss, M.S. Siersbaek, S.F. Schmidt, A.S. Larsen, J.G. Madsen, D.F. Pisani, R. Nielsen, M.M. Aagaard, A. Mathison, M.J. Neville, R. Urrutia, F. Karpe, E.Z. Amri, S. Mandrup, Browning of human adipocytes requires KLF11 and reprogramming of PPARgamma superenhancers, Genes Dev. 29 (2015) 7–22.
[40] L.J. Yuan, Y. Qin, L. Wang, Y. Zeng, H. Chang, J. Wang, B. Wang, J. Wan, S.H. Chen, Q.Y. Zhang, J.D. Zhu, Y. Zhou, M.T. Mi, Capsaicin-containing chili improved postprandial hyperglycemia, hyperinsulinemia, and fasting lipid disorders in women with gestational diabetes mellitus and lowered the incidence of large-for-gestational-age newborns, Clin. Nutr. 35 (2016) 388–393.
[41] J.H. Kang, G. Tsuyoshi, H. Le Ngoc, H.M. Kim, T.H. Tu, H.J. Noh, C.S. Kim, S.Y. Choe, T. Kawada, H. Yoo, R. Yu, Dietary capsaicin attenuates metabolic dysregulation in genetically obese diabetic mice, J. Med. Food 14 (2011) 310–315.
[42] R.K. Baboota, P. Khare, P. Mangal, D.P. Singh, K.K. Bhutani, K.K. Kondepudi, J. Kaur, M. Bishnoi, Dihydrocapsiate supplementation prevented high-fat diet-induced adiposity, hepatic steatosis, glucose intolerance, and gut morphological alterations in mice, Nutr. Res. 51 (2018) 40–56.
[43] J.X. Song, H. Ren, Y.F. Gao, C.Y. Lee, S.F. Li, F. Zhang, L. Li, H. Chen, Dietary capsaicin improves glucose homeostasis and alters the gut microbiota in obese diabetic ob/ob mice, Front. Physiol. 8 (2017) 602.
[44] P. Wang, Z. Yan, J. Zhong, J. Chen, Y. Ni, L. Li, L. Ma, Z. Zhao, D. Liu, Z. Zhu, Transient receptor potential vanilloid 1 activation enhances gut glucagon-like peptide-1 secretion and improves glucose homeostasis, Diabetes 61 (2012) 2155–2165.
[45] K. Chaiyasit, W. Khovidhunkit, S. Wittayalertpanya, Pharmacokinetic and the effect of capsaicin in *Capsicum frutescens* on decreasing plasma glucose level, J. Med. Assoc. Thail. 92 (2009) 108–113.